Peer-reviewed version available at Cancers 2019, 11, 94; doi:10.3390/cancers11010094

Article

Circulating tumor cells develop resistance to TRAIL-induced apoptosis through autophagic removal of death receptor 5: evidence from an *in vitro* model

Julianne D. Twomey [1] and Baolin Zhang [1, *]

[1] Office of Biotechnology Products, Center for Drug Evaluation and Research, Food and Drug Administration, Silver Spring, MD 20993

* Correspondence: Baolin.Zhang@fda.hhs.gov; Tel.: 240-402-6470

Abstract: Circulating tumor cells (CTCs) in the peripheral blood are the precursors to distant metastasis but the underlying mechanisms are poorly understood. This study aims at understanding the molecular features within CTCs in relation to their metastatic potential. Using *in vitro* CTC models, in which breast cancer cell lines are cultured in non-adherent conditions simulating the microenvironment in the blood stream, we found that suspension culture resulted in resistance to TNF-related apoptosis inducing ligand (TRAIL)-mediated cell death. Such a resistance was directly correlated with a reduction in surface and total levels of DR5 protein. In the non-adherent state, cells underwent rapid autophagic flux characterized by an accumulation of autophagosome organelles. Notably, DR5 was translocated to autophagosomes and underwent lysosomal degradation. Our data suggest that CTCs may evade TNF cytokine mediated immune surveillance through downregulation of DR expression. The data warrants further studies in cancer patients to find the status of DRs and other molecular features within primary CTCs in relation to disease progression or chemoresistance.

Keywords: circulating tumor cells; CTCs; breast cancer; metastasis; death receptor; TRAIL; apoptosis; in vitro model;

1. Introduction

Circulating tumor cells (CTCs) are shed into the vasculature from the primary tumor and circulate within the bloodstream. CTCs have the potential to seed distant organs in the body (e.g. bone, liver, lymph nodes, and lungs) where they can grow into new tumors. Several clinical trials have shown that CTC presence in the blood is a surrogate of the risk of progression or death in patients with metastatic solid tumors including breast cancer [1-3]. CTC status is also being explored as a "liquid biopsy" for real-time monitoring of patients' response to therapy [4, 5]. Reports from different groups, however, have shown considerable variation in CTC detection rates and relationship with prognosis or therapy response [6-9], thus limiting their clinical utility as a routine diagnostic tool. At present, a major challenge in the field is to find the molecular signatures within CTC subsets that drive tumor metastasis or resistance to therapy.

CTCs in the peripheral blood are constantly exposed to a perilous environment: a lack of adherent matrix, high fluid shear stress, and cancer targeting immune cells and cytokines [10-12]. The metastatic process is highly vulnerable to these stress signals , with the destruction of most CTCs within minutes by anoikis, a form of apoptosis induced by loss of cell–cell or cell-matrix adhesion [13, 14]. In a rat model of CTCs, only a small proportion of the anoikis resistant population (~ 0.1%) progressed to form micrometastases [15]. Activation of autophagy signaling within CTCs has been proposed as a mechanism though which these cells survive the cumulative stress signals (e.g. detachment, hypoxia) in the circulation thereby contributing to their metastatic potential [13, 16, 17].

Autophagy is characterized by the formation of an autophagosome that can engulf cytoplasmic components as well as selective targets that are tagged with ubiquitin-binding proteins, such as p62 [18], which are degraded following lysosome fusion [19]. Cancer cells can utilize pro-survival autophagy to resist chemotherapies [20], radiation [21], and targeted therapy [22]. This process is tightly regulated by a complex signaling network that involves beclin-1, microtubule-associated protein 1a/1b-light chain 3 (LC3), ATG7, and RAB7/9 as well as other autophagy related proteins.

CTCs' metastatic potential also depends on their susceptibility to immune cells (e.g., macrophage, natural killer cells) and circulating cytokines; including Fas ligand (FasL), tumor necrosis factor α (TNF-α), and TNF-related apoptosis inducing ligand (TRAIL). These cytokines, named death ligands, can induce apoptosis or necroptosis through binding and activation of their cognate death receptors (DRs) Fas, TNF receptor 1 (TNFR1), or DR4/DR5 in target cells, thereby serving a critical mechanism in immunosurveillance and cancer immunity. In many cancer cells, however, activation of this process is hindered due to molecular alterations at several signaling checkpoints, including a deficiency in the expression of DRs on the cell surface. Our lab has previously shown that DR4/DR5 undergo rapid endocytosis and, in some cases, are sequestered into nuclei and autophagosome structures in breast cancer cells [23, 24]. Other factors include overexpression of anti-apoptotic proteins (e.g., IAPs, FLIP, Bcl-2) [25] and/or enhanced cell survival signaling via PI3K/Akt pathway [26]. The observations were made exclusively in primary tumor cells or tumor cell lines, but little is known about the status of DR apoptosis signaling components in CTCs.

CTCs are extremely rare events with a typical frequency of one CTC per billion leukocytes [27], – a confounding factor in CTC isolation and functional characterization. To date, the *CellSearch* CTC detection system is the *only* FDA-approved test for clinical use [28]. The method is designed to capture circulating cells of epithelial origin (CD45-, EpCAM+, and cytokeratins 8, 18+, and/or 19+) in whole blood [2, 3, 8]. However, CTCs are highly heterogenous and the surface markers used in the CellSearch assay are not always present in all CTC populations. Attempts are being made to develop new CTC isolation platforms [29-31] or in vitro CTC models [32-36] . In this study, we developed a long-term suspension cell culture model using human breast cancer cell lines simulating the peripheral blood environment. This model allows a direct comparison between CTCs and their counterpart primary tumor cells being cultured under adherent conditions. Similar approaches have previously been used to examine subpopulations in cancer cell lines [32], death receptor surface localization [33, 34], and chemotherapy resistance [35]. Using in vitro CTC models, we found that breast cancer cells in suspension rapidly undergo autophagic flux resulting in degradation of DR5 and resistance to TRAIL-mediated apoptosis. These data suggest that CTCs may survive TNF cytokine mediated killing through selective downregulation of death receptors in the circulation environment.

2. Results

2.1. Breast cancer cells develop resistance to TRAIL induced apoptosis under non-adherent culture conditions

We aimed to unravel the molecular mechanisms through which CTCs adapt to evading TNF cytokines in the blood stream; including TNF, FasL, and TNF-related apoptosis inducing ligand (TRAIL). To this end, we developed an *in vitro* CTC model wherein human cancer cell lines were cultured in non-adherent conditions simulating the circulating microenvironment. As controls, the same cell lines were also grown under monolayer adherent conditions. Briefly, a panel of three human breast cancer cell lines (MDA-MB-231, MCF7, and ZR75-1) were grown in suspension or

monolayer for 7 days, non-enzymatically dissociated and re-seeded into suspension or monolayer conditions within 96 well plates. Cells were treated with TRAIL at two dosage levels over 24 hours and measured for viability using an MTT assay (Figure 1a). Significant differences in viability between suspension and monolayer cultures were seen following six hours of treatment in MDA-MB-231 cells under the high dosage (50 ng/mL) and by twelve hours of treatment under low dosage (5 ng/mL). At 50 ng/mL TRAIL induced cytotoxicity in the monolayer cultured MDA-MB-231 cells in a time-dependent manner which resulted in 24% (OD 0.24± 0.02) relative viability at 24 hours of incubation. In contrast, MDA-MB-231 cells cultured in suspension conditions underwent an initial reduction in viability which was then maintained around 60% following 12 hours of incubation (OD 0.62±0.01) (Figure 1A). Similar results were seen following 24 hours of rhTRAIL incubation in the ZR75-1 cells (OD 0.37± 0.05 monolayer versus OD 0.70± 0.01 suspension condition) at 50 ng/mL and MCF7 cells (OD 0.65± 0.02 monolayer, versus OD 0.89±0.01) 100 ng/mL. Significant viability differences were seen between the monolayer cells and suspension cultured cells in the ZR75-1 and MCF7 cells by 9 hours and 12 hours under the high dose of TRAIL (50 ng/mL and 100 ng/mL respectively). The delayed apoptosis execution was also shown in the western blot analysis (Figure 1b). TRAIL treatment induced PARP and caspase 3 and 8 cleavage after one hour in monolayer cultured cells compared to three hours in suspension cultured MDA-MB-231 cells, four hours in ZR75-1 cells, and nine hours in MCF7 cells.

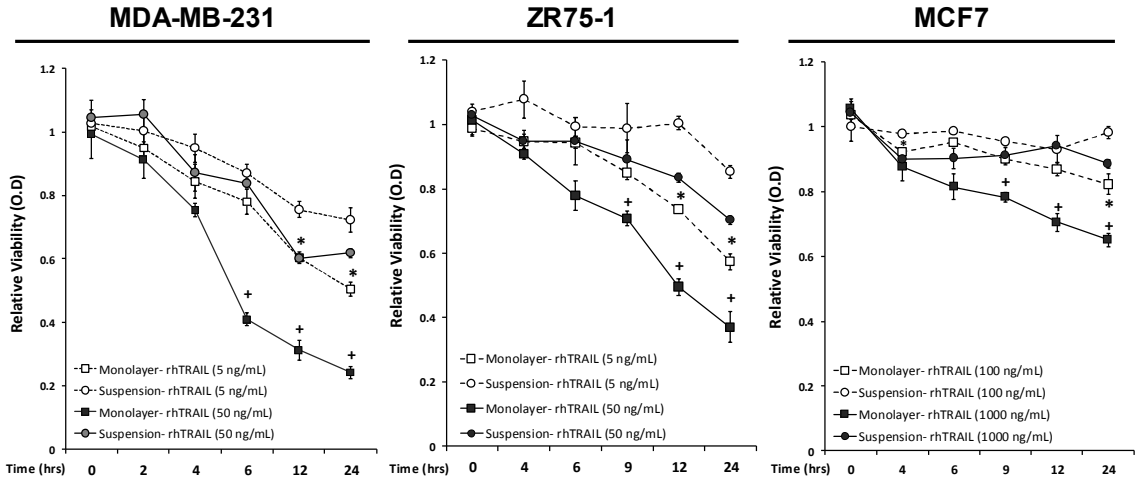

(a)

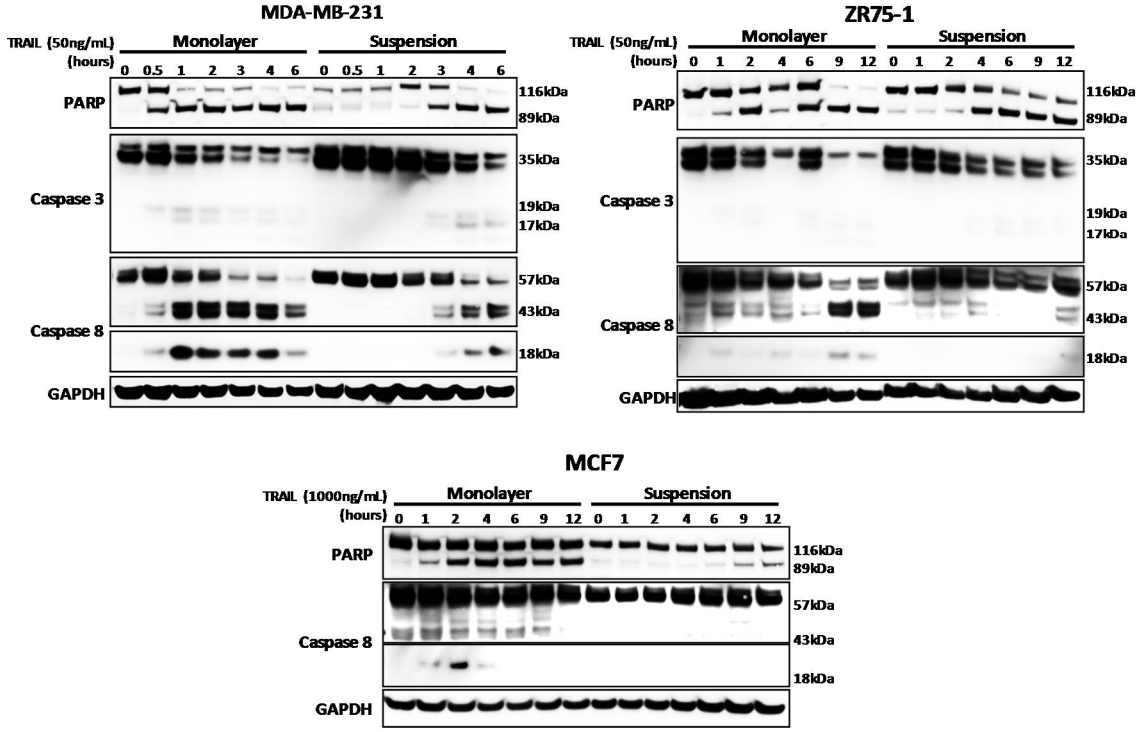

(b)

Figure 1. Breast cancer cells cultured under suspension condition acquire resistance to TRAIL-induced apoptosis. (a) The indicated breast cancer cell lines were cultured under monolayer adherent or non-adherent suspension conditions (see details in Materials & Methods). Cells were seeded at 10,000 cells per well and were then treated with TRAIL (5 ng/mL and 50 ng/mL for MDA-MB-231 and ZR75-1 cell lines; 100 ng/mL and 1000 ng/mL for MCF7 cell lines) over 24 hours. Relative viability was measured at hour intervals using MTT assay and normalized to non-treated controls. Values are means ± SEM of triplicates. (*$p<0.05$ monolayer culture relative to suspension at same time point with rhTRAIL treatment of 5 ng/mL for MDA-MB-231 and ZR75-1 or 100 ng/mL for MCF7 cells; +$p<0.05$ monolayer culture relative to suspension at same time point with rhTRAIL treatment of 50 ng/mL for MDA-MB-231 and ZR75-1 or 1000 ng/mL for MCF7 cells; n=3). (b) Western blot analysis of caspase and PARP cleavage following TRAIL treatment.

2.2. Non-adherent culture selectively decreases DR5 surface and total protein expression

We have previously shown that breast cancer cellular sensitivity to TNF death ligands is correlated with the corresponding death receptor (DR) expression on the plasma membrane [23, 37]. To test this possibility in the non-adherent cultured cells, we performed flow cytometry analysis using antibodies specific to DR4, DR5, Fas, and TNFR1 respectively. Surface expression of DR5, Fas, and TNFR1 was detected in all monolayer cultured cells for MDA-MB-231, ZR75-1, and MCF7 cell lines. Following suspension culture, DR5 surface expression was significantly reduced. By contrast, DR4, TNFR1, and Fas did not show significant changes following suspension culture except for Fas in ZR75-1 cells (Figure S1). We also assessed the expression of other surface receptors including an HLA-Class I Major Histocompatability Complex (MHC), decoy receptors 1 (DcR1) and 2 (DcR2), integrin β1 (ITGβ1), and EGFR. Overall, these receptors were not consistently affected in suspension culture across the cell lines.

Preprints (www.preprints.org) | NOT PEER-REVIEWED | Posted: 19 November 2018 doi:10.20944/preprints201811.0421.v1

Peer-reviewed version available at Cancers 2019, 11, 94; doi:10.3390/cancers11010094

Next, we measured the total protein levels of individual DRs using immunoblot analysis. DR5 and TNFR1 were both significantly reduced over the seven days of suspension culture, with a gradual decrease in total DR5 expression seen in MDA-MB-231 and ZR75-1 cells and a more rapid decrease in MCF7 cells (Figure 2b). DR4 and Fas expression did not show a consistent expression profile over the time or across the samples. At transcriptional level, the mRNA expression of all four DRs did not show significant changes in the two cell lines cultured in suspension, except for MDA-MB-231 cells which showed a slight decrease in DR4 expression (Table 1). These data show that the reduction in DR protein expression likely involve post-translational mechanisms.

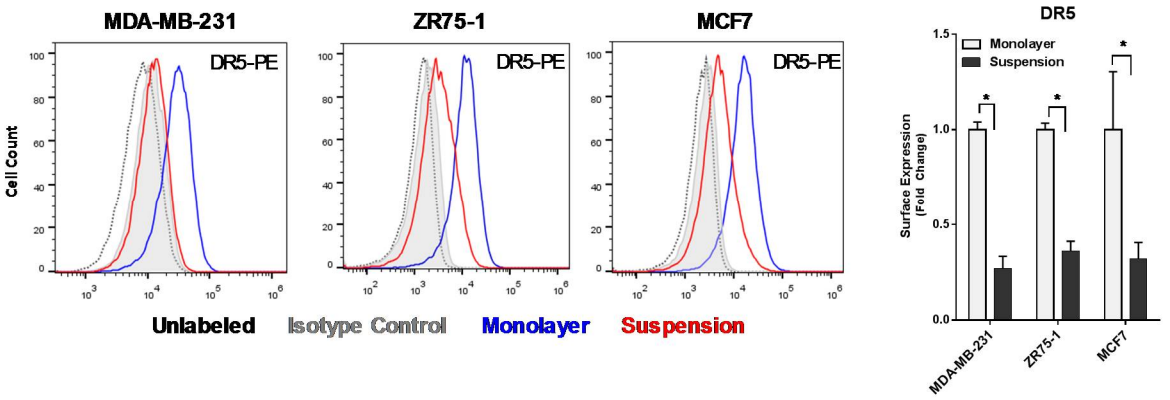

(a)

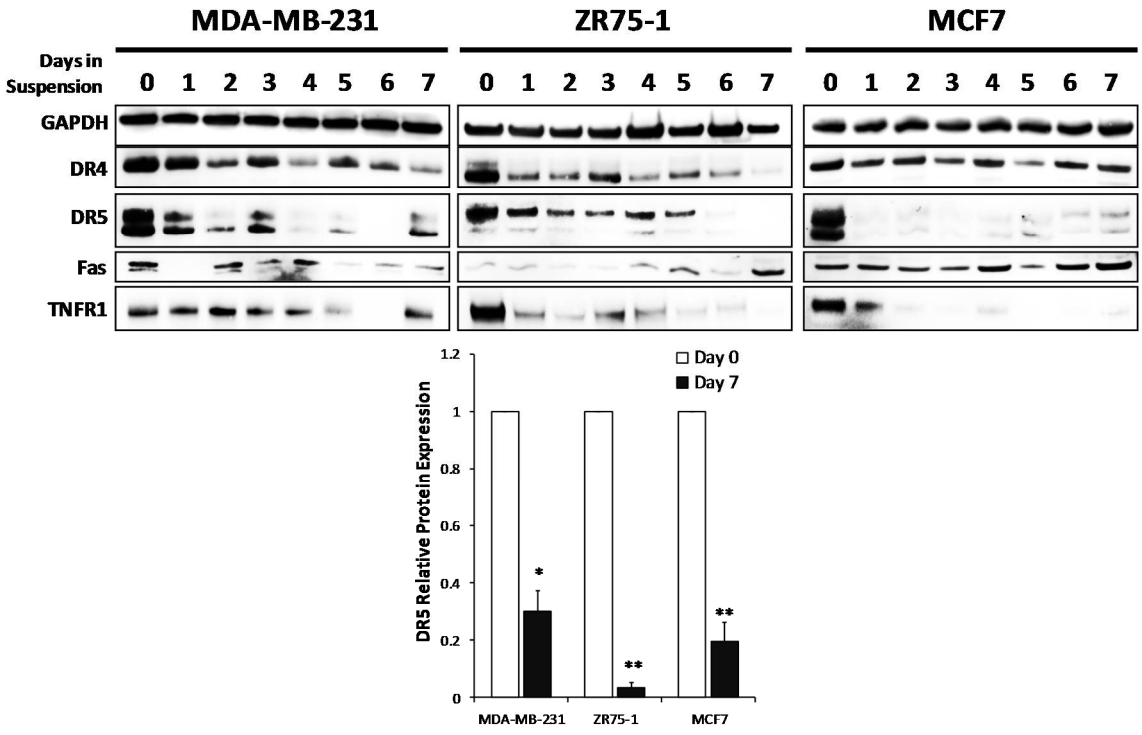

(b)

Figure 2. Surface expression of death receptors are decreased in breast cancer cells under suspension conditions. (A) Surface expression of DR5 was analyzed by flow cytometry on BCCs cultured in monolayer and suspension for seven days. Surface expression was analyzed using Relative Median Fluorescence Intensity (RMFI) of DR5 normalized to the corresponding MFI obtained for monolayer cells (Day 0) (mean ± SEM; *p<0.05; n=3). The reduction in surface level protein is indicated with a median shift of the suspension cultured cells (red line) from monolayer (blue line) towards the isotype (gray shading) and unlabeled control (dotted line). (B) Western blot

analysis of BCC lines cultured in suspension condition and collected each day. Cell lysates were analyzed for DR4, DR5, Fas, and TNFR1 with GAPDH as a loading control. Relative protein expression of DR5 (relative densitometric analysis) to monolayer (day 0). (*p<0.05, **p<0.01 to monolayer; n=3).

Protein	Gene ID	MDA-MB-231 Day 7/ Day 0	MCF7 Day 7/ Day 0
DR4	TNFRSF10a	**-0.711** (0.034)	0.066 (0.835)
DR5	TNFRSF10b	0.281 (0.260)	0.302 (0.386)
Fas	FAS	0.408 (0.293)	0.029 (0.976)
TNFR1	TNFRSF1A	0.151 (0.530)	0.220 (0.188)

(c)

Table 1. Relative gene expression (log_2 ratio (day 7 suspension/ monolayer culture) of DR4, DR5, Fas and TNFR1 determined by the Phalanx Biotech Human OneArray DNA microarray (data shown as log_2 ratio (p-value)).

2.3. Autophagic flux is upregulated in cells cultured in non-adherent conditions.

Previous studies in our lab have shown that autophagic induction causes breast cancer cells to internalize death receptors leading to TRAIL resistance [24]. To examine the status of autophagy, cell samples from suspension culture were analyzed for the autophagy markers of LC3 and the ubiquitin-binding cargo protein p62 (Figure 3a). In suspension culture, all cell lines displayed a significant increase in LC3-II/LC3-I ratio, and a continual decrease of p62 expression. The formation of autophagosomes was confirmed using multispectral imaging flow cytometry analysis (see details in Methods).

The levels of autophagosomes were found to be considerable higher in the cells cultured under suspension compared to respective monolayer cultures in all three cell lines. Monolayer cultures displayed around 2-6% of the cell population having more than seven LC3 puncta per cell, which was determined to be the basal level of autophagy in monolayer culture. There was an increase in this population to around 19-25% following 7 days of suspension culture (Figure 3b: MDA-MB-231: 5.7± 0.4% to 24.5±1.8%, p<0.01; ZR75-1:4.0±0.1% to 18.6±4.1%, p<0.01; MCF7: 1.9±1.1% to 20.9±2.6%, p<0.01).

Further, we analyzed co-localization of LC3-positive puncta with Lysosomal-associated membrane protein 1 (LAMP-1) puncta using bright detail intensity similarity analysis (BDS) for LC3-AF488 and LAMP1-PE. LAMP-1 is a transmembrane glycoprotein that exists in lysosomal membranes. The population of cells that were undergoing autophagic flux (BDS >1.8) increased from monolayer (MDA-MB-231: 1.2±0.6%; ZR75-1: 2.0±0.2%; MCF7: 1.6±0.8%) to suspension culture (MDA-MB-231: 27.3±4.8%; ZR75-1: 13.1±3.7%, p<0.05; MCF7: 32.1±6.4%, p<0.01). These data show that autophagic flux is activated in the non-adherent cultured cells, displaying sustained autophagosome and autolysosome vesicles.

Peer-reviewed version available at Cancers 2019, 11, 94; doi:10.3390/cancers11010094

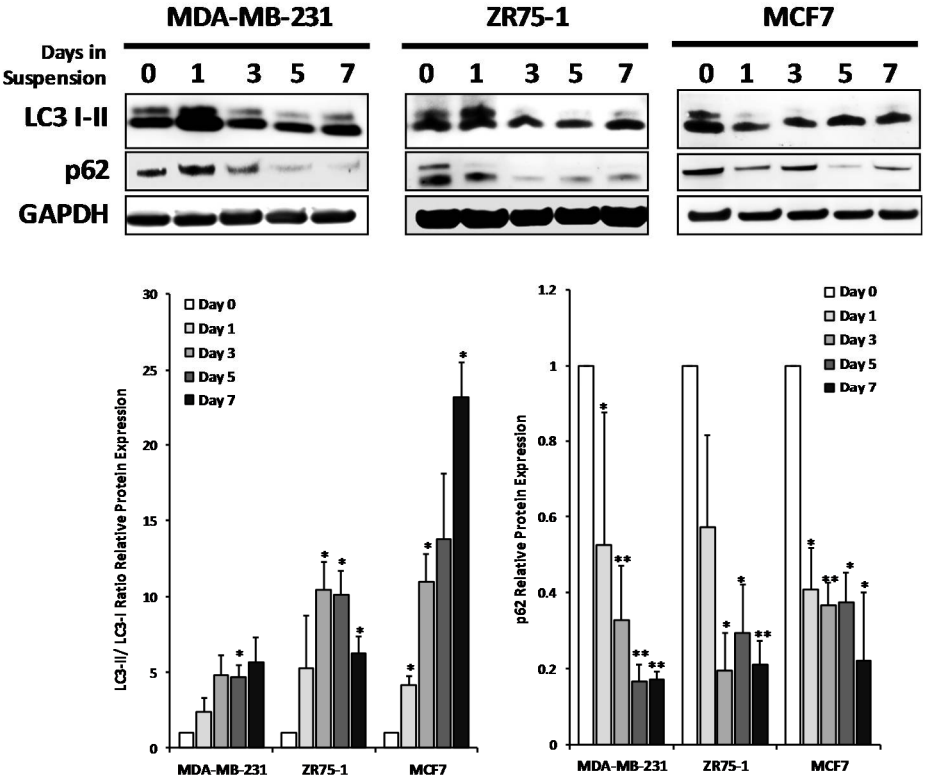

(a)

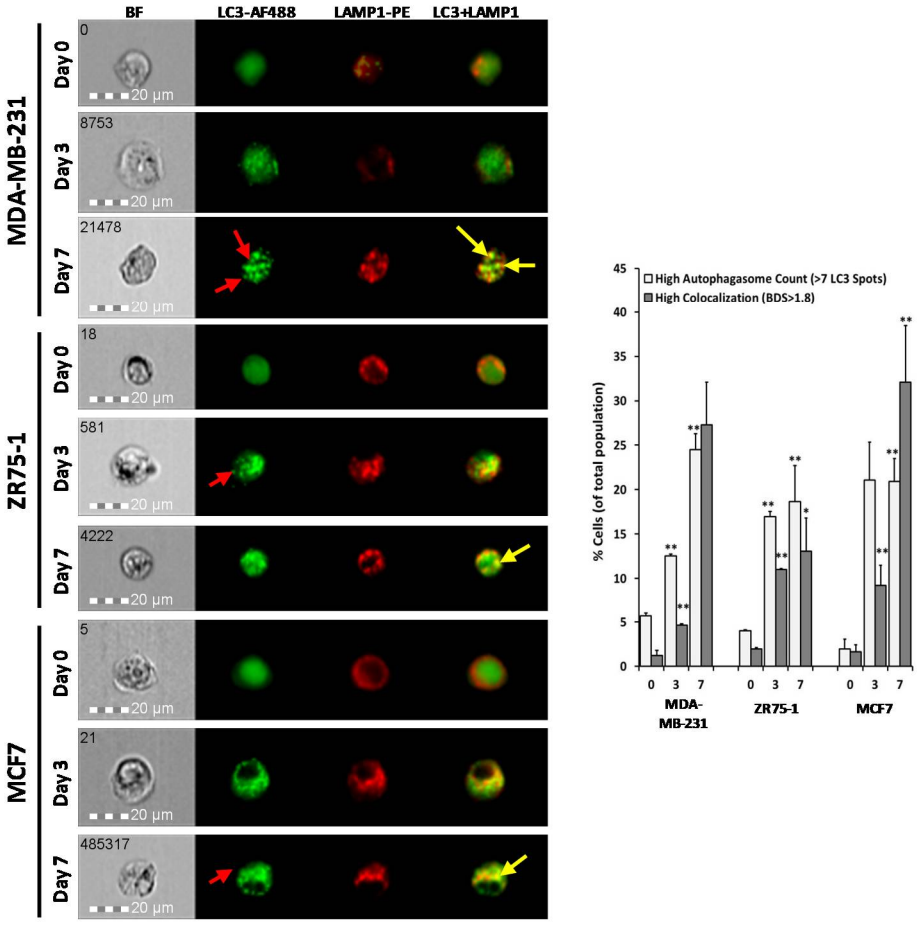

(b)

Figure 3. Non-adherent cultured cells increased autophagic flux as measured by LC3 I-II turnover and autolysosomal formation. (A) Western blot analysis of BCC lines cultured in monolayer or suspension condition up to seven days. Cell lysates were analyzed for LC3-I (top band) and LC3-II (bottom band), p62, and GAPDH. LC3-II to LC3-I relative protein ratio indicating LC3 turnover compared to monolayer (day 0) (mean ± SEM; n=3; *p<0.05). Relative expression of p62 to monolayer cultured cells (mean ± SEM; n=3; *p<0.05). (B) Images of MDA-MB-231, ZR75-1 and MCF7 cells cultured in monolayer or suspension for 3 or 7 days captured using imaging flow cytometry. Shown are brightfield (BF), LC3-AF488 (green), LAMP1-PE (red), and a composite image shown co-localization of LC3 and LAMP1 (yellow). (Single fluorophore controls are shown in Figure S3). Population analysis of cells undergoing autophagy (high autophagosome counts (≥ 7 LC3+ spots per cell)) and autophagic flux (high co-localization of LC3-AF488 and LAMP1-PE (bright detail similarity score ≥ 1.8)) (mean ± SEM; n=3; *p<0.05, **p<0.01 relative to monolayer).

2.4. DR5 is localized to autophagosomes for degradation.

We have previously shown DR5 translocation to autophagosomes in cancer cells under normal growth conditions [24]. To examine this possibility in the non-adherent cultured cells, a co-localization study was performed between DR5-PE and LC3-AF488. Consistent with the immunoblot data, surface levels of DR5 were decreased and the population of double stained cell population was reduced (Figure 4a). Total levels of DR5 and co-localization quantification was performed on the dual-positive population only. Following suspension culture, bright detail similarity significantly increased in all three cell lines, with DR5 staining transitioning from diffuse to more punctate over the course of the seven days. This was further confirmed with confocal microscopy on ZR75-1 cells grown in monolayer or suspension conditions (Figure 4b). Collectively, data suggest that the reduction in DR5 protein level is likely through localization to the autophagosome and subsequent degradation.

Preprints (www.preprints.org) | NOT PEER-REVIEWED | Posted: 19 November 2018 doi:10.20944/preprints201811.0421.v1

Peer-reviewed version available at Cancers 2019, 11, 94; doi:10.3390/cancers11010094

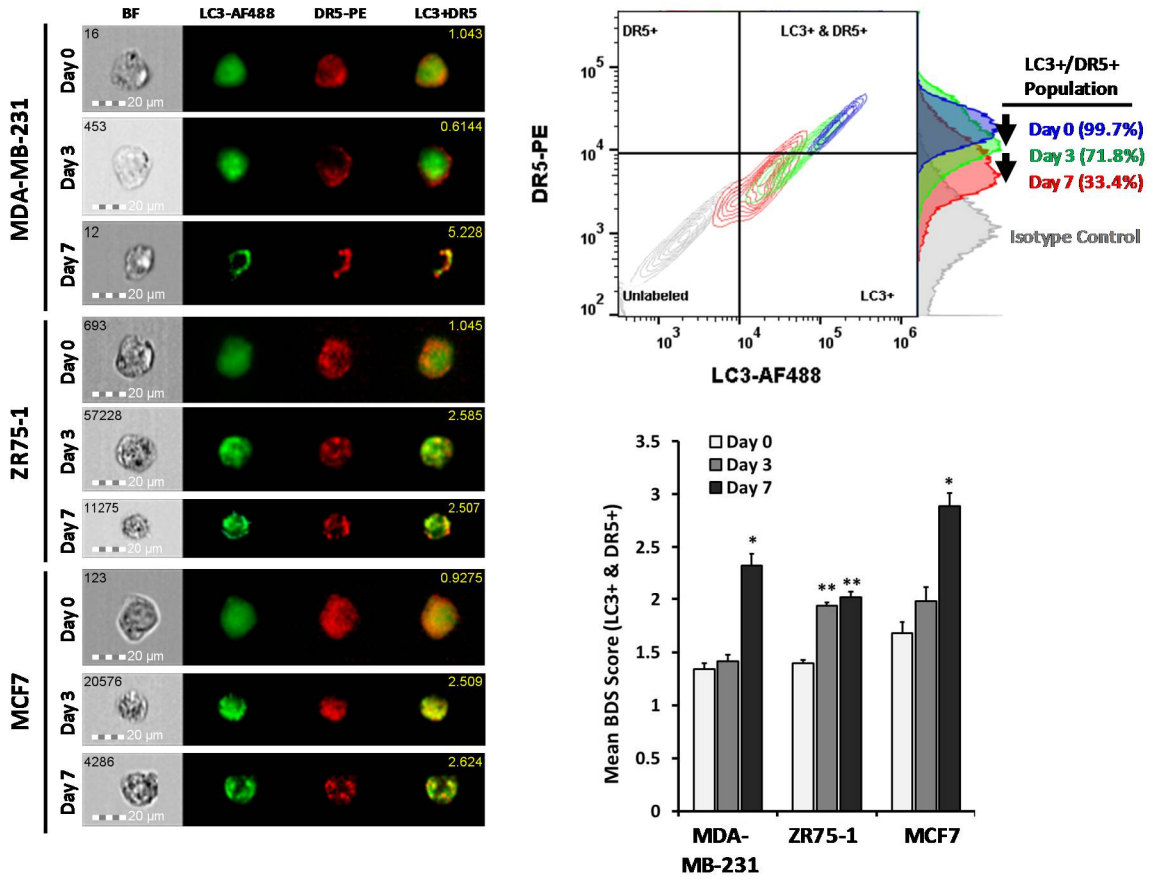

(a)

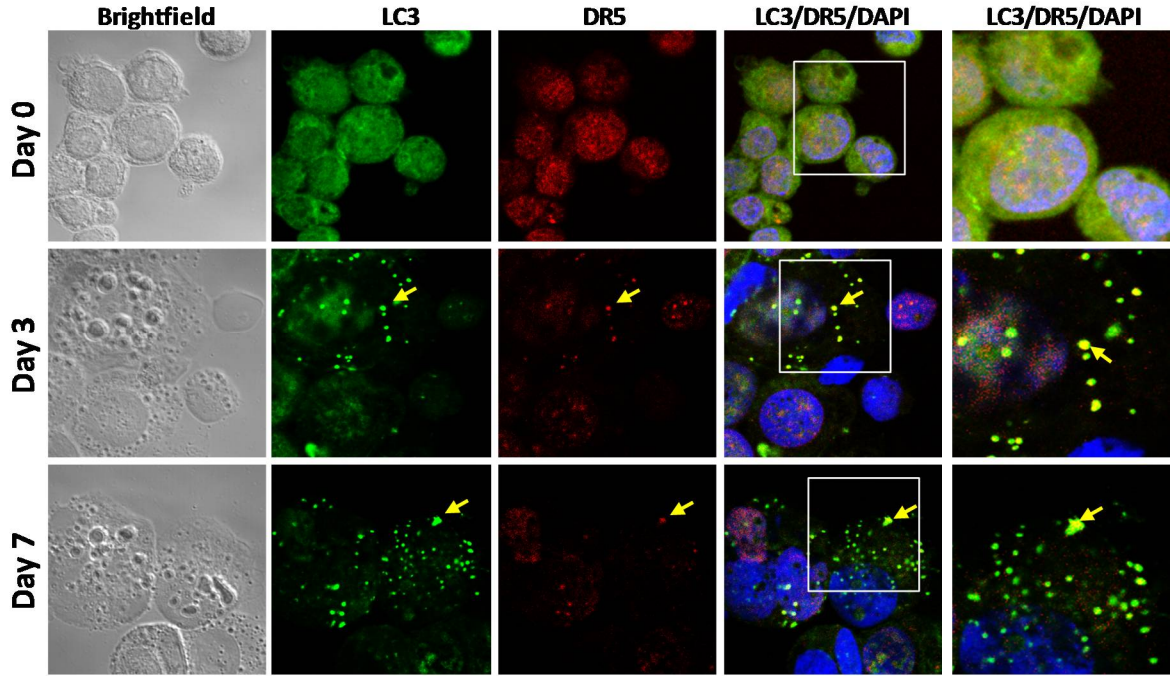

(b)

Figure 4: DR5 localized to autophagosome for degradation under suspension culture. (A) Representative images of MDA-MB-231, ZR75-1 and MCF7 cells cultured in monolayer or suspension for 3 or 7 days captured using imaging flow cytometry. Shown are brightfield (BF), LC3-AF488 (green), DR5-PE (red), and a composite image shown co-localization of LC3 and DR5 (yellow) with the associated bright detail similarity score per cell.

(Single fluorophore controls are shown in figure S3). Bivariate flow cytometry plots of LC3-AF488 and DR5-PE with associated DR5-PE histogram per time point. Population percentages are shown of the dual-positive population. Mean bright detail similarity scores of BCCs cultured in monolayer or suspension culture for 3 or 7 days. BDS scores were calculated on the dual-positive populations only (mean ± SEM; n=3; *p<0.05, **p<0.01 relative to monolayer). (B) Immunocytochemistry and confocal microscopy of cyto-spun ZR75-1 cells cultured in monolayer or suspension for 3 or 7 days. LC3 (AF488, green), DR5 (AF594, red), DAPI, brightfield, and composite micrographs are shown. Yellow arrows indicate co-localized LC3 and DR5. Images taken at 40x.

3. Discussion

As an essential step in the metastatic cascade CTCs must survive the immune defense system involving circulating immune cells and cytokines such as TNF-α, FasL and TRAIL [38]. Here we present a novel mechanism through which CTC subsets may evade TNF cytokine mediated toxicity effects. Using in vitro CTC models, we found that CTC-like cells undergo rapid autophagy flux which targets death receptors (DRs), especially DR5, for autolysosome degradation. The resultant cells become resistant to TRAIL induced apoptosis.

Previous studies have utilized the suspension culture of cancer cell lines to analyze how CTCs undergo changes in proliferation and metabolic pathways [39] as well as in drug sensitivities [40, 41]. In this study, we tested three breast cancer cell lines (MDA-MB-231, ZR75-1, and MCF7) with a known difference in their sensitivity to TNF death ligands under monolayer culture [42]. When cultured in non-adherent condition, all three cell lines showed a delayed apoptotic response to TRAIL with a significant proportion of cells surviving the cytokine mediated killing. This was correlated with a decrease in DR5 protein expression (Figure 4a,b). CTCs have shown reduced surface receptors, as these are not needed within the circulation [36]. It is well documented that matrix detachment increases cellular stress to trigger autophagy in cancer cells [16, 17]. As expected, non-adherent cells displayed rapid autophagic flux as shown by distinct autophagy markers (Figure 3a). Notably, DR5 was found to be co-localized in autophagosome organelles. DR5 mRNA level was not affected; thus, the loss of DR5 protein expression could be attributed to autolysosomal degradation. As shown in monolayer cancer cells [23, 37], a deficiency in the cell surface DR5 is correlated with resistance to TRAIL induced apoptosis.

Our findings also have a potential implication in understanding tumor resistance to DR5 targeted therapies. Due to its proapoptotic activity, DR5 is an attractive target for cancer treatment. There have been several clinical trials testing recombinant human TRAIL and agonistic anti-DR5 monoclonal antibodies. However, these agents have only shown limited clinical efficacy in the completed trials [43-46]. Our data suggest that CTCs may be targeted within the blood stream by endogenous or introduced TRAIL or anti-DR5 molecules, resulting in DR5 deficiency on the cell surface. In support of this notion, we have previously shown that TRAIL or anti-DR5 antibody induces internalization of DR5 from the plasma membrane of monolayer cancer cells [23, 37]. The internalized DR5 can be processed through autophagic degradation in the circulating cells. The resulting CTCs will lose susceptibility to those agents thus resulting in treatment failure. Such a resistance mechanism may be challenged using combination therapy with autophagy inhibitors [24, 47, 48], in light of the evidence that autophagy blockade restores surface DR5 expression thereby augmenting TRAIL-induced apoptotic signaling [24].

In conclusion, we have shown autophagic flux as a mechanism through which tumor cells internalize and degrade death receptors when they are shed from the primary tumor and circulate in the blood stream. The data warrants further studies in cancer patients to find the status of DRs and other molecular features within primary CTCs in relation to disease progression or chemoresistance. The

acquired information can enhance the clinical utility of CTC detection to promote personalized cancer medicine.

4. Materials and Methods

4.1. Cell lines and culture conditions

Human breast cancer cell lines of MCF7 (ATCC, HTB-22), ZR75-1 (ATCC, CRL-1500), and MDA-MB-231 (ATCC, HTB-26) were obtained from the American Type Culture Collection (Manassas, VA) and subcultured per supplier's instructions. MCF7 cells were cultured in Eagle's Minimum Essential Medium (EMEM) (ATCC) supplemented with 10% fetal bovine serum (FBS) (Corning, Corning, NY), and Human Insulin (Invitrogen, Carlsbad, CA). ZR75-1 cells were cultured in RPMI-1640 Medium (ATCC, 30-2001) with 10% FBS and MDA-MB-231 cells were cultured in DMEM/F-12 (1:1) medium (Mediatech, Herndon, VA) containing 5% FBS, 4 mM glutamine, 50 μM β-Mercaptoethanol, and 1mM sodium pyruvate. Cell lines were maintained at 37°C with 5% CO_2. For suspension culture, cells were seeded into Corning Ultra-Low Attachment plates, which inhibits immobilization to the surface. Cells were maintained in suspension with media changes every other day for up to seven days.

4.2. TRAIL Cytotoxicity Assay

Cells were seeded into monolayer or suspension for 7 days at which point cells were isolated using a non-enzymatic dissociation buffer (CellStripper, Invitrogen) and re-seeded into either tissue culture polystyrene or Ultra-Low Attachment 96 well plates at a concentration of 10,000 cells/well. Cells were maintained in complete medium overnight prior to TRAIL treatment. Cells were treated with recombinant human TRAIL (rhTRAIL) (R&D Systems, 375-TEC) at two different doses (10 ng/mL and 100 ng/mL for MDA-MB-231 and ZR75-1 cell lines; 50 ng/mL and 500 ng/mL for MCF7 cell lines). Plates were incubated with rhTRAIL over 24 hours and analyzed for either viability or protein expression at indicated timepoints.

4.3. Cell Viability Assays

Cell viability assays were conducted to determine the effect of rhTRAIL on cells cultured in monolayer and suspension conditions. A standard colorimetric MTT assay was performed to determine the percentage of viable cells. 100 μL of 3-(4,5-dimethylthiazol-2-yl)-2,5-diphenyltetrazoilum bromide (Thiazolul Blue Tetrazolium Bromide) was added to the culture and incubated with the cells for 45 minutes. Cells were then spun down for 10 minutes at 1500 rpm and MTT solution was removed. The resulting crystals were solubilized with DMSO and absorbance was measured using a microplate reader. Absorbance was normalized with respect to non-treated control at each time point and the viability is reported as percentages.

4.4. Flow cytometry detection of surface death receptors

The expression levels of death receptors DR4, DR5, Fas, and TNFR1 were measured on cells cultured in either monolayer or suspension culture for seven days. Cells were dissociated into single cell suspensions using a non-enzymatic dissociation buffer (Cell Stripper). Cells were spun down for 5 minutes and re-suspended at 5.0 x 10^6 cells/mL in blocking solution (1.0% bovine serum albumin, 5.0% normal goat serum (Invitrogen), in PBS). Cells were blocked against non-specific binding for 20 minutes on ice. Cells were then labeled with anti-DR4-PE (IgG_1, R&D Systems, FAB347P), anti-DR5-PE (IgG_{2B}, R&D Systems, FAB6311P), anti-TNFR1-PE (IgG_1, R&D Systems, FAB225P), or anti-Fas-PE ($IgG_{1\kappa}$, BD Pharmigen, 555674) for 45 minutes in the dark on ice according to manufacturer's recommendations. Respective IgG isotype controls were used to determine nonspecific interactions between the antibodies and the cell surface proteins. Cells were washed twice with ice-cold PBS, re-

suspended in 1% BSA-PBS flow cytometry buffer, and analyzed using a BD Accuri C6 flow cytometer. Surface receptor expression was determined by calculating the median fluorescence intensity of the target protein minus the median fluorescence intensity of the corresponding isotype control. All data is shown relative to corresponding monolayer cultured samples of each cell type.

4.5. Western Blotting

Immunoblotting analysis was performed as previously described [24, 37]. Cells lines were cultured in either monolayer or suspension growth conditions and were harvested at specified time points. Cells were washed with PBS and lysed using RIPA lysis buffer with a protease inhibitor. Protein concentrations were determined using the bicinchoninic acid (BCA) protein assay (Pierce, Rockford, IL). Equal amounts of lysis (20 μg) were resolved by electrophoresis using 4-12% NuPAGE Bis-Tris gels and transferred to PVDF membranes (Life Technologies, Carlsbad, CA). Primary antibodies were used at recommended manufacturer's indications (1:500 to 1:1,000). Membranes were stripped using Restore Western Blot Stripping Buffer (Pierce) and re-probed with appropriate antibodies. Immunocomplexes were visualized with chemiluminescence using Immobilon Western Chemiluminescent HRP Substrate. Antibodies specific to human DR4 (D9S1R), DR5 (D4E9), TNFR1 (C25C1), Caspase 3 (8G10), Caspase 8 (1C12), PARP (9542), and p62 (D5E2) were purchased from Cell Signaling Technologies (Danvers, MA). Fas (C-20) was purchased from Santa Cruz Biotechnology (Dallas, Texas). GAPDH (2D4A7) and LC3B/MAP1LC3B (NB100) were purchased from Novus Biologicals (Littleton, CO).

4.6. Gene Expression Analysis

Gene expression was analyzed using the Human OneArray® Plus gene expression profiling service (HOA version 6.2, Phalanx Biotech Group, Inc.). RNA was extracted from MDA-MB-231 and MCF7 cell lines cultured in monolayer or in suspension culture for 7 days. RNA quality was assessed using a NanoDrop ND-1000 with pass critieria of absorbance ratios of A260/A280 ≥1.8 and A260/A230 ≥ 1.5. RNA integrity number (RIN) pass criteria of >6 was used to determine acceptable RNA integrity. Gel electrophoresis was used to evaluate gDNA contamination. The data obtained were analyzed using an Agilent 0.1 XDR Protocol. Gene expression fold changes were calculated by the Rosetta Resolver 7.2 with an error model adjusted by Amersham Pairwise Ration Builder. Differential expression of genes was determined through the selection criteria of $\log2|\text{fold change}| \geq 1$ and $p<0.05$. Data shown are the log2 ratios (suspension compared to monolayer) of each cell type with the corresponding p-value.

4.7. Imaging flow cytometry for autophagic flux analysis

To determine autophagy initiation under suspension culture, multispectral imaging flow cytometry was performed. Cells were dissociated using Cell Stripper, washed once with ice-cold PBS, re-suspended and fixed at a concentration of 10^6 cells/mL in 4% formaldehyde for 10 minutes. Following fixation, cells were washed twice with PBS and then permeabilized using 0.01% Triton-X-100 in 1.0% BSA in PBS solution for 5 minutes. Cells were stained per manufacturer's recommendation with LC3-AF488 (Novus Biologicals, NB-60001384), LAMP1-PE (Novus Biologicals, NBP2-25183), DR5-PE (R&D Systems), in single fluorophore samples or combination samples for co-localization studies. In each experiment, 45,000 cells were acquired using a 12 channel Amnis® FlowSight (EMD Millipore) imaging flow cytometer equipped with 405 nm and 488 nm lasers. Samples were acquired at 40x magnification. Single color controls were also acquired for compensation analysis. IDEAS® (EMD Millipore) software was used for data collection and analysis.

Single cells were identified using a bivariate plot of the cell area and aspect ratio from the bright field imaged population. In focus cells were identified using the Gradient RMS of the bright field images, gating between 35.0 and 72.0 GRMS. Each sample was compensated using single channel controls to minimize spectral spillover. The compensated files were analyzed for LC3 puncta formation and co-localization (bright detail similarity, BDS) on double-positively labeled populations. During autophagosome formation, LC3 is expected to transition from a diffuse cytosolic LC3-I to a clustered autophagosome-membrane bound LC3-II. The LC3-puncta can then be used to find individual autophagosomes. Autophagosome formation was quantified using a function mask to calculate LC3-AF488 bright detail intensity spots (puncta) using a bright detail fluorescence intensity to cell fluorescence ratio of 4.0:1.0 to ensure only autophagosomes are measured without noise from cytoplasmic or non-specific staining. BDI puncta are then counted using the spot-counting feature and a spot radius of less than 1.0 pixel [49-51]. This radius was chosen to best distinguish the individual autophagosomes as there is heterogeneity in size and shape. Histograms were created for the frequency of cells with increasing autophagosome counts. Based on the basal levels of autophagy in breast cancer cell lines cultured in monolayer, cells with more than 7.0 LC3-AF488 puncta per cell were determined as undergoing increased levels of autophagy. The percentage of the cell population that were undergoing increased levels of autophagy were quantified. Autophagic flux was determined by the co-localization between LC3-AF488 (autophagosome marker) and LAMP1-PE (lysosomal marker). Co-localization was calculated using the Bright Detail Similarity (BDS) feature within the IDEAS software. The BDS feature will calculate the pixel location of the bright detail intensities of both LC3-AF488 and LAMP1-PE. A Pearson's correlation of the bright detail intensities' pixel location is calculated, and log transformed into a BDS score to determine the co-localization of two probes between two different channels. Cells undergoing autophagic flux were determined as having a BDS score above 1.8 (Pearson's correlation of $r \approx 0.7$). Co-localization between LC3-AF488 and DR5-PE was determined similarly.

4.8. Immunocytochemistry

For immunocytochemical staining, ZR75-1 cells were cultured in monolayer or suspension for 1, 3, and 7 days. Cells were dissociated with a non-enzymatic dissociation buffer, washed twice, and then re-suspended at a concentration of 0.5 x 10^6 cells/mL. Cells were spun onto microscopy slides using a Thermoscientific Cytospin 4 at 1,000 rpm for three minutes. Cells were then fixed with 4% PFA for 10 minutes, washed twice, permeabilized with 0.01% Triton-X for 5 minutes at room temperature, washed twice, and then blocked using 3% BSA for 20 minutes. Samples were incubated with primary antibodies overnight in blocking solution at 4°C. The following day, slides were washed twice with PBS and incubated for an hour with corresponding conjugated secondary antibodies (goat anti-mouse-AF594 (Life Technologies, A11012) and goat anti-rabbit-AF488 (Life Technologies, A10667). Samples were washed twice and mounted with DAPI-slow fade mounting solution (Vector Laboratories, H-1200). Confocal imaging was performed using a Zeiss LSM880 (Zeiss). Images were obtained at 40x magnification and analyzed using Zen software (Zeiss). Negative controls were unlabeled samples and secondary antibody only stained samples.

4.9. Statistical Analysis

Statistical analysis for cell viability, flow cytometry, western blotting, and co-localization studies were performed using GraphPad Prism 6 (GraphPad Software). Statistical comparisons were determined using one-way ANOVA and un-paired t-test with a Welch's correction. All assays were

completed with an N≥3. Statistical significance is shown as either *p<0.05 or **p<0.01 as indicated in the results.

Supplementary Materials: The following are available online at www.mdpi.com/xxx/s1, **Figure S1.** Flow cytometry detection of death receptors and cell surface proteins. **Figure S2.** Quantification of death receptor protein expression. **Figure S3.** MIFC single fluorophore controls. **Figure S4.** Representative MIFC spot count histograms for LC3-AF488 puncta (autophagosomes).

Author Contributions: Conceptualization, J.T. and B.Z.; Methodology, J.T.; Formal Analysis, J.T. and B.Z.; Investigation, J.T.; Data Curation, J.T.; Writing- original draft preparation, J.T. and B.Z.; Writing- review and editing, J.T. and B.Z.; Supervision, B.Z.; Funding Acquisition, B.Z.;

Funding: This study was supported by the US FDA intramural research funding.

Conflicts of Interest: The authors declare no conflict of interest.

References

1. León-Mateos, L., Casas, H., Abalo, A., Vieito, M., Abreu, M., Anido, U., Gómez-Tato, A., López, R., Abal, M., and Muinelo-Romay, L. "Improving Circulating Tumor Cells Enumeration and Characterization to Predict Outcome in First Line Chemotherapy Mcrpc Patients." *Oncotarget* 8, no. 33 (2017): 54708-21. doi: 10.18632/oncotarget.18025
2. Smerage, J. B., Barlow, W. E., Hortobagyi, G. N., Winer, E. P., Leyland-Jones, B., Srkalovic, G., Tejwani, S., Schott, A. F., O'Rourke, M. A., Lew, D. L., Doyle, G. V., Gralow, J. R., Livingston, R. B., and Hayes, D. F. "Circulating Tumor Cells and Response to Chemotherapy in Metastatic Breast Cancer: Swog S0500." *Journal of clinical oncology : official journal of the American Society of Clinical Oncology* 32, no. 31 (2014): 3483-89. doi: 10.1200/JCO.2014.56.2561
3. Cristofanilli, M. "Circulating Tumor Cells, Disease Progression, and Survival in Metastatic Breast Cancer." *Seminars in Oncology* 33 (2006): 9-14. doi: https://doi.org/10.1053/j.seminoncol.2006.03.016
4. Ng, S. P., Bahig, H., Wang, J., Cardenas, C. E., Lucci, A., Hall, C. S., Meas, S., Sarli, V. N., Yuan, Y., Urbauer, D. L., Ding, Y., Ikner, S., Dinh, V., Elgohari, B. A., Johnson, J. M., Skinner, H. D., Gunn, G. B., Garden, A. S., Phan, J., Rosenthal, D. I., Morrison, W. H., Frank, S. J., Hutcheson, K. A., Mohamed, A. S. R., Lai, S. Y., Ferrarotto, R., MacManus, M. P., and Fuller, C. D. "Predicting Treatment Response Based on Dual Assessment of Magnetic Resonance Imaging Kinetics and Circulating Tumor Cells in Patients with Head and Neck Cancer (Predict-Hn): Matching 'Liquid Biopsy' and Quantitative Tumor Modeling." *BMC Cancer* 18, no. 1 (2018): 903-03. doi: 10.1186/s12885-018-4808-5
5. Keup, C., Mach, P., Aktas, B., Tewes, M., Kolberg, H.-C., Hauch, S., Sprenger-Haussels, M., Kimmig, R., and Kasimir-Bauer, S. "Rna Profiles of Circulating Tumor Cells and Extracellular Vesicles for Therapy Stratification of Metastatic Breast Cancer Patients." *Clinical Chemistry* 64, no. 7 (2018): 1054-62. doi: 10.1373/clinchem.2017.283531
6. Yan, W.-T., Cui, X., Chen, Q., Li, Y.-F., Cui, Y.-H., Wang, Y., and Jiang, J. "Circulating Tumor Cell Status Monitors the Treatment Responses in Breast Cancer Patients: A Meta-Analysis." *Scientific reports* 7 (2017): 43464-64. doi: 10.1038/srep43464
7. Politaki, E., Agelaki, S., Apostolaki, S., Hatzidaki, D., Strati, A., Koinis, F., Perraki, M., Saloustrou, G., Stoupis, G., Kallergi, G., Spiliotaki, M., Skaltsi, T., Lianidou, E., Georgoulias, V., and Mavroudis, D. "A Comparison of Three Methods for the Detection of Circulating

Tumor Cells in Patients with Early and Metastatic Breast Cancer." *Cellular Physiology and Biochemistry* 44, no. 2 (2017): 594-606. doi: 10.1159/000485115

8. Janni, W. J., Rack, B., Terstappen, L. W. M. M., Pierga, J.-Y., Taran, F.-A., Fehm, T., Hall, C., de Groot, M. R., Bidard, F.-C., Friedl, T. W. P., Fasching, P. A., Brucker, S. Y., Pantel, K., and Lucci, A. "Pooled Analysis of the Prognostic Relevance of Circulating Tumor Cells in Primary Breast Cancer." *Clinical Cancer Research* 22, no. 10 (2016): 2583. doi:

9. Hartkopf, A. D., Wagner, P., Wallwiener, D., Fehm, T., and Rothmund, R. "Changing Levels of Circulating Tumor Cells in Monitoring Chemotherapy Response in Patients with Metastatic Breast Cancer." *Anticancer Research* 31, no. 3 (2011): 979-84. doi:

10. Kim, Y.-N., Koo, K. H., Sung, J. Y., Yun, U.-J., and Kim, H. "Anoikis Resistance: An Essential Prerequisite for Tumor Metastasis." *International Journal of Cell Biology* 2012 (2012). doi: 10.1155/2012/306879

11. Mitchell, M. J., and King, M. R. "Fluid Shear Stress Sensitizes Cancer Cells to Receptor-Mediated Apoptosis Via Trimeric Death Receptors." *New journal of physics* 15 (2013): 015008. doi: 10.1088/1367-2630/15/1/015008

12. Rejniak, K. A. "Circulating Tumor Cells: When a Solid Tumor Meets a Fluid Microenvironment." *Advances in experimental medicine and biology* 936 (2016): 93-106. doi: 10.1007/978-3-319-42023-3_5

13. Paoli, P., Giannoni, E., and Chiarugi, P. "Anoikis Molecular Pathways and Its Role in Cancer Progression." *Biochimica et Biophysica Acta (BBA) - Molecular Cell Research* 1833, no. 12 (2013): 3481-98. doi: https://doi.org/10.1016/j.bbamcr.2013.06.026

14. Laguinge, L. M., Samara, R. N., Wang, W., El-Deiry, W. S., Corner, G., Augenlicht, L., Mishra, L., and Jessup, J. M. "Trail Dr5 Receptor Mediates Anoikis in Human Colorectal Carcinoma Cell Lines." *Cancer Research* 68, no. 3 (2008): 909. doi:

15. Weiss, L., Mayhew, E., Rapp, D. G., and Holmes, J. C. "Metastatic Inefficiency in Mice Bearing B16 Melanomas." *British journal of cancer* 45, no. 1 (1982): 44-53. doi:

16. Fung, C., Lock, R., Gao, S., Salas, E., and Debnath, J. "Induction of Autophagy During Extracellular Matrix Detachment Promotes Cell Survival." *Molecular Biology of the Cell* 19, no. 3 (2008): 797-806. doi: 10.1091/mbc.E07-10-1092

17. Avivar-Valderas, A., Bobrovnikova-Marjon, E., Diehl, J. A., Bardeesy, N., Debnath, J., and Aguirre-Ghiso, J. A. "Regulation of Autophagy During Ecm Detachment Is Linked to a Selective Inhibition of Mtorc1 by Perk." *Oncogene* 32, no. 41 (2013): 4932-40. doi: 10.1038/onc.2012.512

18. Lippai, M., and Low, P. "The Role of the Selective Adaptor P62 and Ubiquitin-Like Proteins in Autophagy." *BioMed Research International* 2014 (2014): 11. doi: 10.1155/2014/832704

19. Yang, X., Yu, D.-D., Yan, F., Jing, Y.-Y., Han, Z.-P., Sun, K., Liang, L., Hou, J., and Wei, L.-X. "The Role of Autophagy Induced by Tumor Microenvironment in Different Cells and Stages of Cancer." *Cell & Bioscience* 5 (2015): 14. doi: 10.1186/s13578-015-0005-2

20. Ojha, R., Jha, V., Singh, S. K., and Bhattacharyya, S. "Autophagy Inhibition Suppresses the Tumorigenic Potential of Cancer Stem Cell Enriched Side Population in Bladder Cancer." *Biochimica et Biophysica Acta (BBA) - Molecular Basis of Disease* 1842, no. 11 (2014): 2073-86. doi: https://doi.org/10.1016/j.bbadis.2014.07.007

21. Apel, A., Herr, I., Schwarz, H., Rodemann, H. P., and Mayer, A. "Blocked Autophagy Sensitizes Resistant Carcinoma Cells to Radiation Therapy." *Cancer Research* 68, no. 5 (2008): 1485. doi:

22. Eritja, N., Chen, B.-J., Rodríguez-Barrueco, R., Santacana, M., Gatius, S., Vidal, A., Martí, M. D., Ponce, J., Bergadà, L., Yeramian, A., Encinas, M., Ribera, J., Reventós, J., Boyd, J., Villanueva, A., Matias-Guiu, X., Dolcet, X., and Llobet-Navàs, D. "Autophagy Orchestrates Adaptive Responses to Targeted Therapy in Endometrial Cancer." *Autophagy* 13, no. 3 (2017): 608-24. doi: 10.1080/15548627.2016.1271512

23. Zhang, Y., and Zhang, B. "Trail Resistance of Breast Cancer Cells Is Associated with Constitutive Endocytosis of Death Receptors 4 and 5." *Molecular Cancer Research* 6, no. 12 (2008): 1861. doi:

24. Di, X., Zhang, G., Zhang, Y., Takeda, K., Rivera Rosado, L. A., and Zhang, B. "Accumulation of Autophagosomes in Breast Cancer Cells Induces Trail Resistance through Downregulation of Surface Expression of Death Receptors 4 and 5." *Oncotarget* 4, no. 9 (2013). doi:

25. Huang, Y., Yang, X., Xu, T., Kong, Q., Zhang, Y., Shen, Y., Wei, Y., Wang, G., and Chang, K.-J. "Overcoming Resistance to Trail-Induced Apoptosis in Solid Tumor Cells by Simultaneously Targeting Death Receptors, C-Flip and Iaps." *International Journal of Oncology* 49, no. 1 (2016): 153-63. doi: 10.3892/ijo.2016.3525

26. Xu, J., Zhou, J.-Y., Wei, W.-Z., and Wu, G. S. "Activation of the Akt Survival Pathway Contributes to Trail Resistance in Cancer Cells." *PLOS ONE* 5, no. 4 (2010): e10226. doi: 10.1371/journal.pone.0010226

27. Sun, Y.-F., Yang, X.-R., Zhou, J., Qiu, S.-J., Fan, J., and Xu, Y. "Circulating Tumor Cells: Advances in Detection Methods, Biological Issues, and Clinical Relevance." *Journal of Cancer Research and Clinical Oncology* 137, no. 8 (2011): 1151-73. doi: 10.1007/s00432-011-0988-y

28. Ferreira, M. M., Ramani, V. C., and Jeffrey, S. S. "Circulating Tumor Cell Technologies." *Molecular Oncology* 10, no. 3 (2016): 374-94. doi: https://doi.org/10.1016/j.molonc.2016.01.007

29. Kallergi, G., Politaki, E., Alkahtani, S., Stournaras, C., and Georgoulias, V. "Evaluation of Isolation Methods for Circulating Tumor Cells (Ctcs)." *Cellular Physiology and Biochemistry* 40, no. 3-4 (2016): 411-19. doi: 10.1159/000452556

30. Au, S. H., Edd, J., Stoddard, A. E., Wong, K. H. K., Fachin, F., Maheswaran, S., Haber, D. A., Stott, S. L., Kapur, R., and Toner, M. "Microfluidic Isolation of Circulating Tumor Cell Clusters by Size and Asymmetry." *Scientific reports* 7, no. 1 (2017): 2433. doi: 10.1038/s41598-017-01150-3

31. Adams, D. L., Zhu, P., Makarova, O. V., Martin, S. S., Charpentier, M., Chumsri, S., Li, S., Amstutz, P., and Tang, C.-M. "The Systematic Study of Circulating Tumor Cell Isolation Using Lithographic Microfilters." *RSC advances* 9 (2014): 4334-42. doi: 10.1039/C3RA46839A

32. Calvet, C. Y., André, F. M., and Mir, L. M. "The Culture of Cancer Cell Lines as Tumorspheres Does Not Systematically Result in Cancer Stem Cell Enrichment." *PLOS ONE* 9, no. 2 (2014): e89644. doi: 10.1371/journal.pone.0089644

33. Chandrasekaran, S., Marshall, J. R., Messing, J. A., Hsu, J.-W., and King, M. R. "Trail-Mediated Apoptosis in Breast Cancer Cells Cultured as 3d Spheroids." *PLOS ONE* 9, no. 10 (2014): e111487. doi: 10.1371/journal.pone.0111487

34. Liu, G.-C., Zhang, J., Liu, S.-G., Gao, R., Long, Z.-F., Tao, K., and Ma, Y.-F. "Detachment of Esophageal Carcinoma Cells from Extracellular Matrix Causes Relocalization of Death Receptor 5 and Apoptosis." *World Journal of Gastroenterology : WJG* 15, no. 7 (2009): 836-44. doi: 10.3748/wjg.15.836
35. Smit, L., Berns, K., Spence, K., Ryder, W. D., Zeps, N., Madiredjo, M., Beijersbergen, R., Bernards, R., and Clarke, R. B. "An Integrated Genomic Approach Identifies That the Pi3k/Akt/Foxo Pathway Is Involved in Breast Cancer Tumor Initiation." *Oncotarget* 7, no. 3 (2016): 2596-610. doi: 10.18632/oncotarget.6354
36. Nanou, A., Crespo, M., Flohr, P., De Bono, J., and Terstappen, L. "Scanning Electron Microscopy of Circulating Tumor Cells and Tumor-Derived Extracellular Vesicles." *Cancers* 10, no. 11 (2018): 416. doi:
37. Chen, J.-J., Jennifer Shen, H. C., Rivera Rosado, L. A., Zhang, Y., Di, X., and Zhang, B. "Mislocalization of Death Receptors Correlates with Cellular Resistance to Their Cognate Ligands in Human Breast Cancer Cells." *Oncotarget* 3, no. 8 (2012): 833-42. doi:
38. Zamai, L., Ponti, C., Mirandola, P., Gobbi, G., Papa, S., Galeotti, L., Cocco, L., and Vitale, M. "Nk Cells and Cancer." *The Journal of Immunology* 178, no. 7 (2007): 4011-16. doi: 10.4049/jimmunol.178.7.4011
39. Park, J. Y., Jeong, A. L., Joo, H. J., Han, S., Kim, S.-H., Kim, H.-Y., Lim, J.-S., Lee, M.-S., Choi, H.-K., and Yang, Y. "Development of Suspension Cell Culture Model to Mimic Circulating Tumor Cells." *Oncotarget* 9, no. 1 (2018): 622-40. doi: 10.18632/oncotarget.23079
40. Gencoglu, M. F., Barney, L. E., Hall, C. L., Brooks, E. A., Schwartz, A. D., Corbett, D. C., Stevens, K. R., and Peyton, S. R. "Comparative Study of Multicellular Tumor Spheroid Formation Methods and Implications for Drug Screening." *ACS biomaterials science & engineering* 4, no. 2 (2018): 410-20. doi: 10.1021/acsbiomaterials.7b00069
41. Gravelle, P., Jean, C., Familiades, J., Decaup, E., Blanc, A., Bezombes-Cagnac, C., Laurent, C., Savina, A., Fournié, J.-J., and Laurent, G. "Cell Growth in Aggregates Determines Gene Expression, Proliferation, Survival, Chemoresistance, and Sensitivity to Immune Effectors in Follicular Lymphoma." *The American Journal of Pathology* 184, no. 1 (2014): 282-95. doi: https://doi.org/10.1016/j.ajpath.2013.09.018
42. Chen, J.-J., Knudsen, S., Mazin, W., Dahlgaard, J., and Zhang, B. "A 71-Gene Signature of Trail Sensitivity in Cancer Cells." *Molecular Cancer Therapeutics* 11, no. 1 (2012): 34-44. doi: 10.1158/1535-7163.mct-11-0620
43. Herbst, R. S., Eckhardt, S. G., Kurzrock, R., Ebbinghaus, S., O'Dwyer, P. J., Gordon, M. S., Novotny, W., Goldwasser, M. A., Tohnya, T. M., Lum, B. L., Ashkenazi, A., Jubb, A. M., and Mendelson, D. S. "Phase I Dose-Escalation Study of Recombinant Human Apo2l/Trail, a Dual Proapoptotic Receptor Agonist, in Patients with Advanced Cancer." *Journal of Clinical Oncology* 28, no. 17 (2010): 2839-46. doi: 10.1200/JCO.2009.25.1991
44. Hotte, S. J., Hirte, H. W., Chen, E. X., Siu, L. L., Le, L. H., Corey, A., Iacobucci, A., MacLean, M., Lo, L., Fox, N. L., and Oza, A. M. "A Phase 1 Study of Mapatumumab (Fully Human Monoclonal Antibody to Trail-R1) in Patients with Advanced Solid Malignancies." *Clinical Cancer Research* 14, no. 11 (2008): 3450-55. doi: 10.1158/1078-0432.ccr-07-1416
45. Forero-Torres, A., Shah, J., Wood, T., Posey, J., Carlisle, R., Copigneaux, C., Luo, F. R., Wojtowicz-Praga, S., Percent, I., and Saleh, M. "Phase I Trial of Weekly Tigatuzumab, an

Agonistic Humanized Monoclonal Antibody Targeting Death Receptor 5 (Dr5)." *Cancer biotherapy & radiopharmaceuticals* 25, no. 1 (2010): 13-19. doi: 10.1089/cbr.2009.0673

46. Camidge, D. R. "Apomab: An Agonist Monoclonal Antibody Directed against Death Receptor 5/Trail-Receptor 2 for Use in the Treatment of Solid Tumors." *Expert Opinion on Biological Therapy* 8, no. 8 (2008): 1167-76. doi: 10.1517/14712598.8.8.1167

47. Han, J., Hou, W., Goldstein, L. A., Lu, C., Stolz, D. B., Yin, X.-M., and Rabinowich, H. "Involvement of Protective Autophagy in Trail Resistance of Apoptosis-Defective Tumor Cells." *Journal of Biological Chemistry* 283, no. 28 (2008): 19665-77. doi: 10.1074/jbc.M710169200

48. Monma, H., Iida, Y., Moritani, T., Okimoto, T., Tanino, R., Tajima, Y., and Harada, M. "Chloroquine Augments Trail-Induced Apoptosis and Induces G2/M Phase Arrest in Human Pancreatic Cancer Cells." *PLOS ONE* 13, no. 3 (2018): e0193990. doi: 10.1371/journal.pone.0193990

49. Rajan, R., Karbowniczek, M., Pugsley, H. R., Sabnani, M. K., Astrinidis, A., and La-Beck, N. M. "Quantifying Autophagosomes and Autolysosomes in Cells Using Imaging Flow Cytometry." *Cytometry Part A* 87, no. 5 (2015): 451-58. doi: 10.1002/cyto.a.22652

50. Phadwal, K., Alegre-Abarrategui, J., Watson, A. S., Pike, L., Anbalagan, S., Hammond, E. M., Wade-Martins, R., McMichael, A., Klenerman, P., and Simon, A. K. "A Novel Method for Autophagy Detection in Primary Cells." *Autophagy* 8, no. 4 (2012): 677-89. doi: 10.4161/auto.18935

51. Pugsley, H. R. "Quantifying Autophagy: Measuring Lc3 Puncta and Autolysosome Formation in Cells Using Multispectral Imaging Flow Cytometry." *Methods* 112 (2017): 147-56. doi: http://doi.org/10.1016/j.ymeth.2016.05.022